Civil Engineering
Engenharia Civil

Numerical analysis of reinforced concrete asymmetric cross-section beams under oblique bending

http://dx.doi.org/10.1590/0370-44672018720070

Bruno Tasca de Linhares[1]
https://orcid.org/0000-0002-8968-9777

[1]Universidade Comunitária da Região de Chapecó - ACEA, Curso de Engenharia Civil, Chapecó - Santa Catarina - Brasil.
bruno.linhares@unochapeco.edu.br

Abstract

The problem of symmetric cross-section beams under oblique bending is well known to professional designers and academy. In fact, symmetric elements make up most of the cross-sections defined in design. The case of the asymmetric cross-sections is, however, little discussed in literature, but is a particular problem, especially in bridge girder design, joined *in loco*. The asymmetry generates oblique bending when the load is out of the principal inertia planes. Thus, this article presents a comparison of results between a numerical solution of the elastic curve differential equations, and a Finite Element Model (FEM), for a 10m span reinforced concrete beam, with gutter-shaped asymmetric cross-section, whose only load is its own weight. The required geometric properties were determined by the Green Theorem. From theoretical study, the elastic curve differential equations were obtained, in the vertical and horizontal directions. The angular displacement conditions at the beginning of the span were obtained by the Virtual Work Method. After integration using the Runge-Kutta Method, the maximum displacements in the vertical and horizontal directions, in the middle span, are 0.904cm and 0.611cm, respectively (1.091cm resultant displacement). The Finite Element Model was performed in ANSYS 9.0. The resultant displacement of the numerical model was 1.16cm. Concurrently, the axial stresses were studied in the middle span. The stress results for both approaches (Runge-Kutta and FEM) differed by no more than 8.72%. These results guarantee reliability to the Runge-Kutta integration, from a design view point, to the proposed problem analysis in Serviceability Limit State.

Keywords: asymmetric cross-sections. elastic curve. Runge-Kutta Method. Finite Element Method.

1. Introduction

Most structural elements in civil construction (beams, columns) consist of straight bars with symmetric cross-section. The bending moments are treated separately in both directions (vertical and horizontal) and the bending axial stresses are superimposed, since the element has axes of symmetry.

In the case of the symmetric cross-sections, if a bending moment is applied in the direction of an axis of symmetry, the element displacement will occur in the plane perpendicular to that bending moment, and the Elastic Neutral Axis (ENA) will coincide with the bending moment.

The asymmetric cross-sections are frequently applied, for example, in roofing purlins, where steel profiles have unconventional cross-sections. These situations do not characterize a great problem, considering the low loads and spans to which they are submitted.

An important problem for asymmetric cross-sections is the case of precast concrete girders with unconventional geometry, which are joined at the construction site to form a symmetric section. Thus, during their casting and prestressing, and even the transport to the construction site, they are asymmetric cross-section girders subject to oblique bending. Besides the prestressing, other loads that also cause oblique flexion in this type of element are the dead load and other live loads.

For these situations, the transverse displacement occurs in 2 directions for any applied load; in a direction perpendicular to the Elastic Neutral Axis. The ENA direction is also unknown in the problem.

This work presents the study of a gutter-shaped cross-section beam (asymmetric) under its dead load, applied in vertical direction, determination of the geometric properties using Green Theorem, flexure axial stresses and transversal displacements by numerical method (Runge-Kutta). A finite element model is introduced to corroborate the results.

2. Materials and methods

2.1 Green Theorem

According to Kreyszig (2009), the Green Theorem transforms double integrals in a region R of the xy plane into contour integrals in the C contour of this region, according to Equation 1:

$$\iint_R \left(\frac{\partial F_2}{\partial x} - \frac{\partial F_1}{\partial y}\right) dxdy = \oint_C F_1\, dx + F_2\, dy \tag{1}$$

This equation can be worked for discrete straight fragments in the plane and, thus, it is possible to obtain the equations that determine the geometric properties of any cross-section, from the coordinates of their vertices. The geometric properties, area, static moments in x and y axes, moments of inertia in x and y axes, and product of inertia are given by Equations (2) to (7), respectively (KREYSZIG, 2009):

$$A = \frac{1}{2}\sum_{i=1}^{N}(x_{i+1} + x_i)\,\Delta y \tag{2}$$

$$S_x = \frac{1}{6}\sum_{i=1}^{N}\{6x_i y_i + 3x_i\Delta y + \Delta x.[3y_i + 2\Delta y]\}\,\Delta y \tag{3}$$

$$S_y = \frac{1}{6}\sum_{i=1}^{N}\{3{x_i}^2 + \Delta x.[3x_i + \Delta x]\}\,\Delta y \tag{4}$$

$$I_x = \sum_{i=1}^{N}\left\{x_i\left[{y_i}^2 + y_i\Delta y + \frac{\Delta y^2}{3}\right] + \Delta x.\left[\frac{{y_i}^2}{2} + \frac{2y_i\Delta y}{3} + \frac{\Delta y^2}{4}\right]\right\}\Delta y \tag{5}$$

$$I_y = \frac{1}{3}\sum_{i=1}^{N}\left\{{x_i}^3 + \Delta x\left[\frac{3{x_i}^2}{2} + x_i\Delta x + \frac{\Delta x^2}{4}\right]\right\}\Delta y \tag{6}$$

$$I_{xy} = \frac{1}{2}\sum_{i=1}^{N}\left\{{x_i}^2\left[y_i + \frac{\Delta y}{2}\right] + \Delta x\left[x_i y_i + \frac{2x_i\Delta y}{3}\right] + \Delta x^2\left[\frac{y_i}{3} + \frac{\Delta y}{4}\right]\right\}\Delta y \tag{7}$$

With the definition of a matrix of coordinates of the cross-section N vertices, and using the previous equations, the direction of the principal axes of inertia can be found.

2.2 Axial stresses - Fundaments

According to Oden and Ripperger (1981), the axial stresses in a coplanar curved beam, are obtained from the force resultants acting in the cross-section. For this, the strain of a "y" generic position in the cross-section is studied (Figure 1).

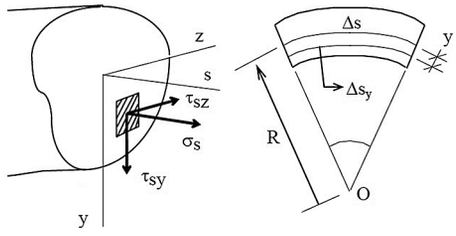

Figure 1
Axial and tangential stresses for curved beams (ODEN; RIPPERGER, 1981).

The validity of the hypothesis of plane sections (Bernoulli Hypothesis) is assumed and that the displacements in the cross-section are contained in a plane. One has, therefore, in the s-direction (Equation 8):

$$u = \bar{a} + \bar{b}.y + \bar{c}.z \tag{8}$$

The constants $\bar{a}$, $\bar{b}$ and $\bar{c}$ are functions of s (cross-section axis). The ratio between the lengths Δs and Δs_y is given by Equation 9, from the analysis of Figure 1:

$$\frac{ds}{ds_y} = \frac{1}{1-\frac{y}{R}} \tag{9}$$

The axial strain in the generic y-position in the cross-section is given by Equation 10:

$$\varepsilon_{sy} = \frac{du}{ds_y} = \frac{d\bar{a}}{ds}\frac{ds}{ds_y} + \frac{d\bar{b}}{ds}\frac{ds}{ds_y}y + \frac{d\bar{c}}{ds}\frac{ds}{ds_y}z = (a + b.y + c.z)\frac{ds}{ds_y} \tag{10}$$

After differentiating the function u (Equation 8), and applying the chain rule with Equation 9, the axial strain of the generic y-coordinate is obtained. By Hooke's Law for elastic materials, and neglecting the Poisson effects, the axial stress in the y-coordinate is given (Equation 11):

$$\sigma_{sy} = E.\varepsilon_{sy} = \frac{E}{1-\frac{y}{R}}(a + b.y + c.z) \tag{11}$$

With Equation 11, the resultants of axial stresses (N_s axial force, M_y and M_z moments) can be reached by integration along the cross-section area. With the aid of Maclaurin series to simplify the integrals of the resultants, the constants a, b and c of Equation 11 are determined. By eliminating the subscript y of this equation, the axial stresses of flexo-compression/tension are given by Equation 12:

$$\sigma_s = \frac{N_s}{A} - \frac{M_z}{AR} + \frac{M_z J_y - M_y J_{yz}}{J_y J_z - {J_{yz}}^2}\frac{y}{1-\frac{y}{R}} + \frac{M_y J_z - M_z J_{yz}}{J_y J_z - {J_{yz}}^2}\frac{z}{1-\frac{y}{R}} \tag{12}$$

In this equation J_y, J_z and J_{yz} are constants of inertia of the cross-section, Equation 13:

$$J_y = \int_A \frac{z^2 dA}{1-\frac{y}{R}} \quad J_z = \int_A \frac{y^2 dA}{1-\frac{y}{R}} \quad J_{yz} = \int_A \frac{yz dA}{1-\frac{y}{R}} \tag{13}$$

By making $R \to \infty$, they are particularized for straight bars, and the constants of inertia become moments of inertia and product of inertia (see Equation 14). With Equation 14, the direction of the Elastic Neutral Axis (ENA) and the axial stresses can be found.

$$\sigma_s(z,y) = \frac{N_s}{A} + \frac{M_z I_y - M_y I_{yz}}{I_y I_z - {I_{yz}}^2}y + \frac{M_y I_z - M_z I_{yz}}{I_y I_z - {I_{yz}}^2}z \tag{14}$$

2.3 Elastic curve – Fundaments

Considering isotropic elastic-linear material, the principle of superimposition can be applied. The cross-section displacement is a superimposition of the baricentric axis displacement (u_0), shortening of the cross-section vertical coordinates by wedging (u_1) and displacement by cross-section rotation around the y and z axes (u_2), according to Equation 15:

$$u = u_0 + u_1 + u_2 \tag{15}$$

Figures 2 to 3 illustrate the displacements.

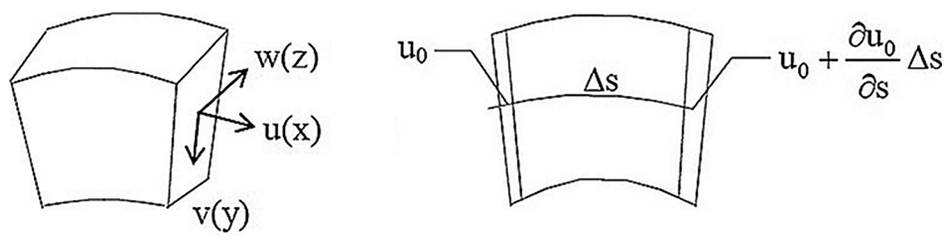

Figure 2
Axes and displacement u_0 (ODEN; RIPPERGER, 1981).

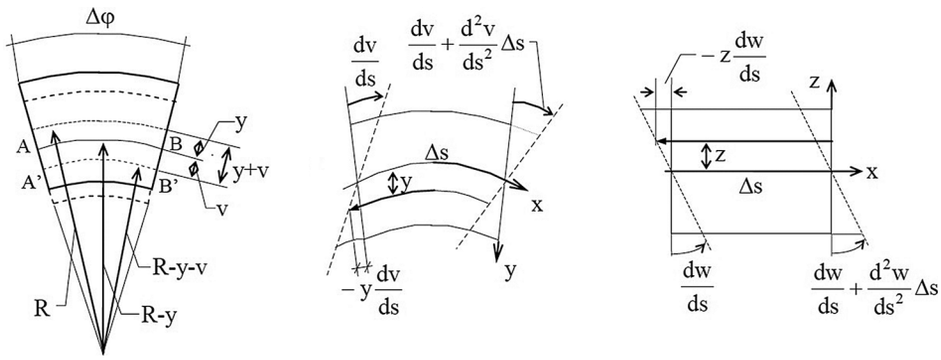

Figure 3
Displacements u_1 e u_2
(ODEN; RIPPERGER, 1981).

For a generic vertical *y*-position, the Equation 15 can be particularized according to:

$$u = u_{0y} + u_{1y} + u_{2y} \tag{16}$$

Thus, the cross-section *y*-position strain is given by the derivative of the Equation 16 with respect to the sy fiber, according to Equation 17:

$$\varepsilon_{sy} = \frac{du}{ds_y} = \frac{du_{0y}}{ds_y} + \frac{du_{1y}}{ds_y} + \frac{du_{2y}}{ds_y} = \varepsilon_{s0} + \varepsilon_{s1} + \varepsilon_{s2} \tag{17}$$

To the first term of Equation 17, the chain rule can be applied, since u0y ($u_0(s(s_y))$), in analogy to Equation 9, resulting:

$$\varepsilon_{s0} = \frac{du_{0y}}{ds_y} = \frac{du_{0y}}{du_0}\frac{du_0}{ds}\frac{ds}{ds_y} = \left(1 - \frac{y}{R}\right)\frac{du_0}{ds}\frac{1}{\left(1 - \frac{y}{R}\right)} = \frac{du_0}{ds} \tag{18}$$

For the second term of Equation 17, the strain ε_{s1} can be obtained from the left-hand side of Figure 3. Thus, Equation 19:

$$\varepsilon_{s1} = \frac{du_{1y}}{ds_y} = \frac{(R - y - v)\Delta\Phi - (R - y)\Delta\Phi}{(R - y)\Delta\Phi} = \frac{-v}{R - y} = \frac{-y.v}{\left(1 - \frac{y}{R}\right)R^2} - \frac{v}{R} \tag{19}$$

For the third term of Equation 17, the right-hand side of Figure 3 is taken as the composition for displacement u_2. Therefore, Equation 20:

$$\varepsilon_{s2} = \frac{du_{2y}}{ds_y} = \frac{du_{2y}}{ds}\frac{ds}{ds_y} = \frac{1}{\left(1 - \frac{y}{R}\right)}\left(-y\frac{d^2v}{ds^2} - z\frac{d^2w}{ds^2}\right) \tag{20}$$

Finally, the sum of the strains given by Equations 18, 19 and 20 is equal to the axial stress σ_s (given by Equation 12) divided by the modulus of elasticity (Hooke's Law):

$$\frac{du_0}{ds} - \frac{v}{R} - \left(\frac{d^2v}{ds^2} + \frac{v}{R^2}\right)\frac{y}{1 - \frac{y}{R}} - \frac{d^2w}{ds^2}\frac{z}{1 - \frac{y}{R}} = \frac{\sigma_s}{E} \tag{21}$$

Working the terms, along with Equation 12, the differential equations of the elasticity curve for a coplanar curved beam under oblique bending are given by the Equations of (22): Working the terms, along with Equation 12, the differential equations of the elasticity curve for a coplanar curved beam under oblique bending are given by the Equations of (22):

$$\begin{cases} \dfrac{du_0}{ds} - \dfrac{v}{R} = \dfrac{N_s}{AE} - \dfrac{M_z}{RAE} \\ \dfrac{d^2v}{ds^2} + \dfrac{v}{R^2} = -\dfrac{M_zI_y - M_yI_{yz}}{E\left(I_yI_z - {I_{yz}}^2\right)} \\ \dfrac{d^2w}{ds^2} = -\dfrac{M_yI_z - M_zI_{yz}}{E\left(I_yI_z - {I_{yz}}^2\right)} \end{cases} \tag{22}$$

The first Equation of (22) refers to the barycentric elasticity curve; that is, displacements along the element axis. The second equation is the elasticity curve in the y-direction; and the third one, in the z-direction. These equations were simplified in this study by making $R \rightarrow \infty$ for straight bars. The first Equation of (22) was neglected in the displacement calculations in this study. The equations of (22) suggest that the displacement will occur in two directions, even with loading in only one direction.

Note that if the cross section is symmetric ($I_{yz} = 0$), the last two equations of (22) are reduced to the classical differential equations of the elastic curve.

2.4 Elastic curve – case study

Herein is presented the case of a gutter-shaped cross-section reinforced concrete beam, therefore asymmetric, simply supported and with a 10m span, submitted only to its own weight (Figure 4). Due to the asymmetry of the cross-section, this is a case of oblique bending. The reinforced concrete specific weight is $\gamma = 25kN/m^3$ and its modulus of elasticity is defined as E = 26070MPa. Thus, the own weight dead load to which the beam is subjected is 13.6kN/m, applied in the y-direction in the beam geometric center.

Figure 4 illustrates its cross-section (dimensions in centimeters), its principal inertia axes direction (θp), and the geometric properties determined by the Green Method (programmed in MathCad), from a coordinate matrix of its vertices.

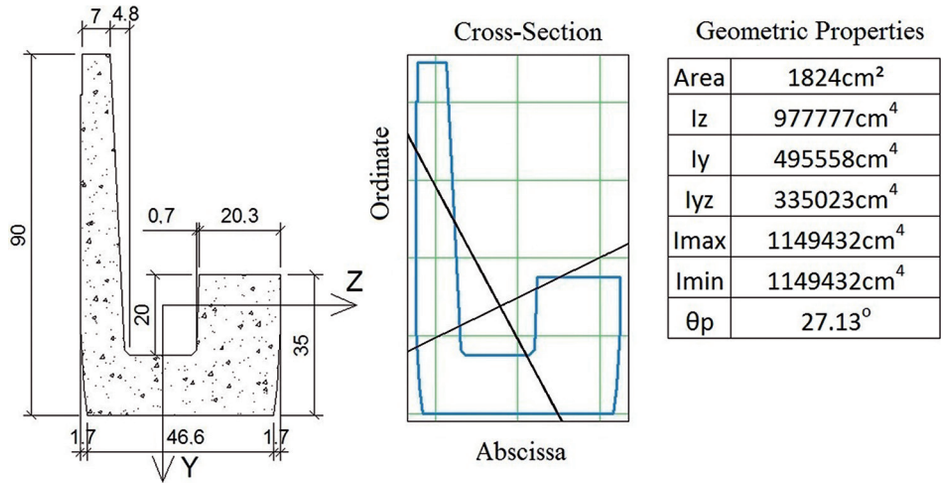

Geometric Properties

Area	1824cm²
Iz	977777cm^4
Iy	495558cm^4
Iyz	335023cm^4
Imax	1149432cm^4
Imin	1149432cm^4
θp	27.13°

Figure 4
Cross-section, principal axes of inertia and geometric properties.

With the own weight dead load and the span (10m), the equation of the bending moment in the z-direction was defined, for a section in a generic position (x) in the element's longitudinal axis, as: $M_z(x) = -6.8x^2 + 68x$ [$kN.m$]; the M_y moment, in the other direction, is null.

Through the geometric properties and the bending moment equations, one can integrate the second and third equations of (22) with the Runge-Kutta Method, and obtain the final elasticity curves in both directions.

However, since two-order differential equations are involved, two boundary conditions are required for their resolution (BURDEN, FAIRES, 2013). Since the beam is simply supported, one condition is the null displacement at x=0m in both directions ($v(0)$=0m and $w(0)$=0m). The second condition is the elastic curve slope (angular displacement) at x=0m, which can be determined by the Virtual Work Method (Figure 5).

By neglecting the effect of shear effort, the elastic curve slope is determined from the definition of a unitary virtual moment in the position x=0m (SORIANO; LIMA, 2006). The angular displacement by bending moment of real loads is obtained from the analysis of Equations 22 of the elasticity curve for asymmetric sections.

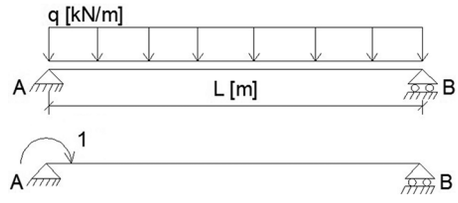

Figure 5
Virtual work method –Angular displacement.

Thus, the virtual bending moment equation and the final equations of the Virtual Work Method (VWM) for the initial elasticity curve slope of the asymmetric cross-sections are given by Equations 23 to 25, respectively (MARTHA, 2010).

$$\bar{M} = 1 - \frac{x}{L} \qquad (23)$$

$$v'(0) = \int_0^L -\frac{M_z I_y - M_y I_{yz}}{E\left(I_y I_z - {I_{yz}}^2\right)}(\bar{M})dx \qquad (24)$$

$$w'(0) = \int_0^L -\frac{M_y I_z - M_z I_{yz}}{E\left(I_y I_z - {I_{yz}}^2\right)}(\bar{M})dx \tag{25}$$

In this way, all the necessary data to perform the differential equations integration by Runge-Kutta are given. The initial slope conditions resulted: $v'(0)$=-0.002893rad and $w'(0)$=-0.001955rad.

The Runge-Kutta Method, for higher-order equations, is given by a simplification of the original equation for two first-order equations, and is summarized in Equation 26. The term h is the integration step; in this study, its value was h=0.1m (PRESS *et al.*, 2007).

$$\begin{cases} \boldsymbol{y'' + by' + cy = 0} \\ \boldsymbol{y'_{1,n+1} = f_1(x, y_{1,n}, y_{2,n}) = y_{2,n}} \\ \boldsymbol{y'_{2,n+1} = f_2(x, y_{1,n}, y_{2,n}) = -by_{2,n} - cy_{1,n}} \\ \boldsymbol{k1 = h\begin{bmatrix} f_1(x, y_{1,n}, y_{2,n}) \\ f_2(x, y_{1,n}, y_{2,n}) \end{bmatrix}} \\ \boldsymbol{k2 = h\begin{bmatrix} f_1(x + 0.5h, y_{1,n} + 0.5k1_1, y_{2,n} + 0.5k1_2) \\ f_2(x + 0.5h, y_{1,n} + 0.5k1_1, y_{2,n} + 0.5k1_2) \end{bmatrix}} \\ \boldsymbol{k3 = h\begin{bmatrix} f_1(x + 0.5h, y_{1,n} + 0.5k2_1, y_{2,n} + 0.5k2_2) \\ f_2(x + 0.5h, y_{1,n} + 0.5k2_1, y_{2,n} + 0.5k2_2) \end{bmatrix}} \\ \boldsymbol{k4 = h\begin{bmatrix} f_1(x + 0.5h, y_{1,n} + k3_1, y_{2,n} + k3_2) \\ f_2(x + 0.5h, y_{1,n} + k3_1, y_{2,n} + k3_2) \end{bmatrix}} \\ \boldsymbol{y_{n+1} = \begin{bmatrix} y_{1,n} \\ y_{2,n} \end{bmatrix} + \frac{1}{6}(k1 + 2k2 + 2k3 + k4)} \end{cases} \tag{26}$$

These equations were programmed in MathCad, in the *y* and *z* directions, to obtain the displacement curves. A 3D model in finite element, with isoparametric elements of 8 nodes and 3 degrees of freedom per node, was defined to corroborate these results (BATHE, 1996). The linear own weight dead load was also applied to the numerical model geometric center.

3. Results

3.1 Axial stresses of oblique bending – Finite element model

The finite element model was performed with the software ANSYS 9.0 (element SOLID45). Figure 6 illustrates the bending axial stresses for the own weight dead load in a cross-section of the middle span.

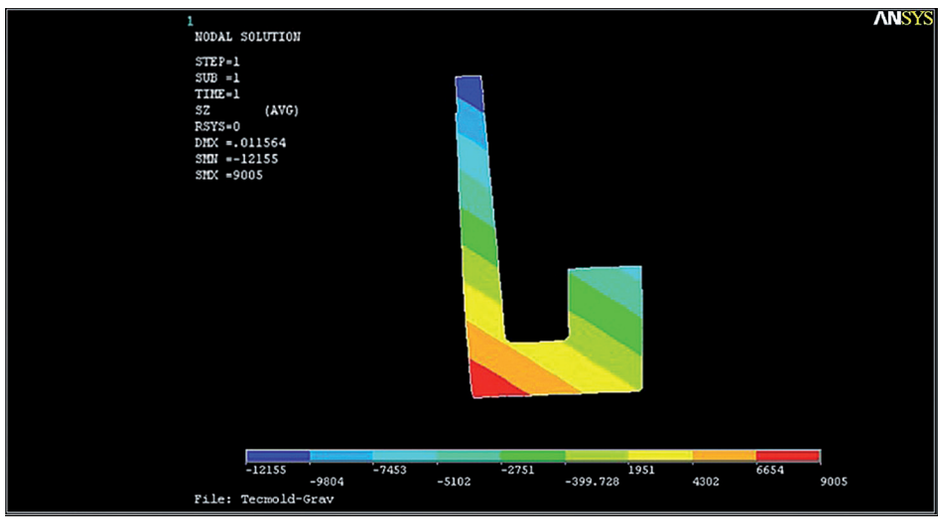

Figure 6
Axial stresses of oblique bending – span center [kn/m²].

It is observed that the numerical compression axial stress in the upper center of the beam left flap is -12155kN/m²; at the same point, the analytical axial stress (obtained with Equation 14), is σ_s(-16.7cm, -62.6cm)=-11610kN/m². The numerical compression axial stress in the upper center of the beam right flap is -5102kN/m²; at the same point, the analytical axial stress is σ_s(19.2cm, -7.6cm)=-4657kN/m². The numerical tension axial stress at the lower left corner is 9005kN/m²; at the same point, the analytical axial stress is σ_s(-18.94cm, 27.4cm)=9097kN/m².

3.2 Elastic curve displacements – Finite element model

The numerical displacements in the middle span are given in Figures 7 and 8.

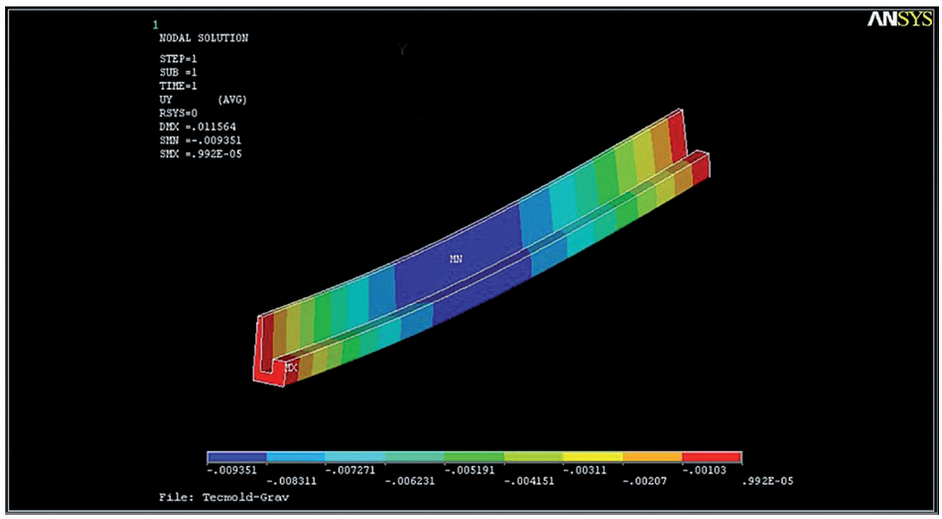

Figure 7
Displacements in
y-direction [m] – v_{max} = -0.935cm.

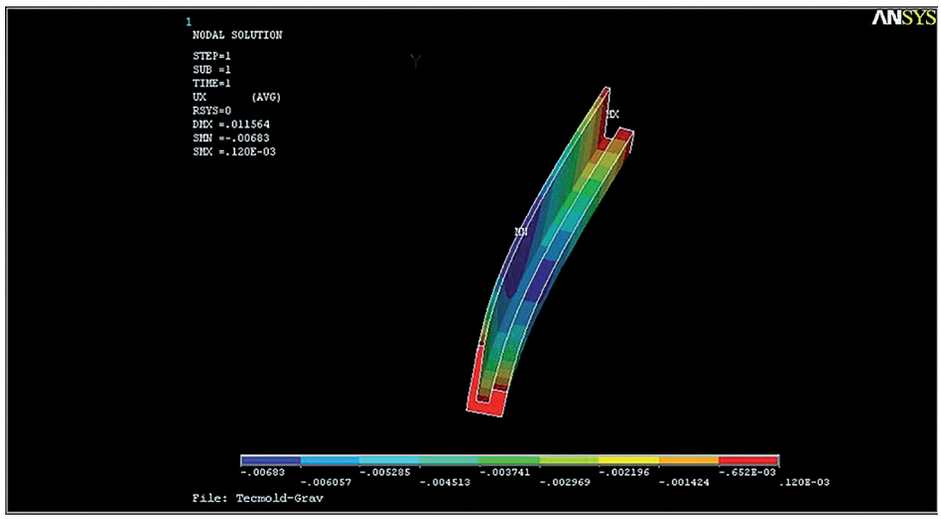

Figure 8
Displacements in
z-direction [m] – w_{max} = -0.683cm.

It is observed that the displacements in the middle span resulted: v(5m)=-0.935cm; w(5m)=-0.683cm. The resultant displacement is (in modulus) 1.16cm. It should be noted that the ANSYS 9.0 axis convention is different from the one adopted in the analytical method.

Figure 9 shows the resulting displacements from the integration of the differential equations by Runge-Kutta. The displacements were: v(5m)=0.904cm and w(5m)=-0.611cm. Thus, the resultant displacement is 1.091cm.

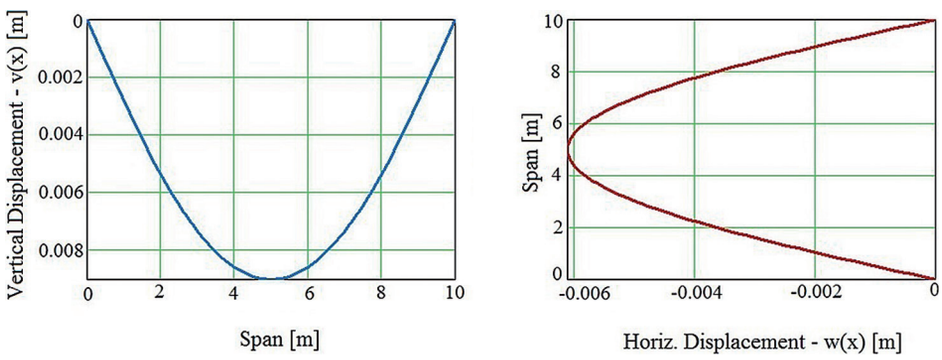

Figure 9
Displacements in the
y and z directions – Runge-Kutta Method.

4. Discussion

The result analysis, in terms of axial stresses, shows that the analytical equation approximated well the values of the numerical model. The maximum difference observed at the points analyzed was 8.72%. From the axial stress diagram (Figure 6), it can be seen that the Elastic Neutral Axis (ENA) is inclined, following the direction of the presented axial stress boundaries. In fact, working the Equation 14 to zero, it results, approximately, in a 34° slope

for the ENA with respect to the horizontal axis (clockwise), which coincides with the stress diagram from Figure 6.

It is noted in the numerical model, as expected, that there were displacements in the horizontal and vertical directions. An inspection of the Equations of (22), had already predicted this effect.

5. Conclusion

This research aimed to highlight the structural effects that occur in an element with asymmetric cross-section. The cross-section's lack of symmetry produces, even for loading in only one direction, displacements in both directions, as well as a slope on the Elastic Neutral Axis (ENA). Generally, structural analysis programs neglect this effect, presenting only the displacement in the load direction, independently of the cross-section characteristics. Therefore, it is important to verify the asymmetry effects, especially in elements submitted to prestressing, considering that this type of structure is verified in the Serviceability Limit State (SLS), through axial stress and displacements control.

The asymmetry effect is evident when the angular displacement in a bar by the Virtual Work Method is studied (Equations 24 and 25). The real displacement is a function of the cross-section product of inertia and moments of inertia in both directions. Thus, the angular displacement given by Equation 24, is only the y-component of the resultant angular displacement in both directions.

The analytical displacement, in the middle span, resulted: $v(5m)$=0.904cm, $w(5m)$= -0.611cm, with resultant displacement of 1.091cm. This results in an angle of 55.94° (~56° counter-clockwise) with the horizontal axis. Since the Elastic Neutral Axis (ENA) has an angle of ~34° clockwise with respect to the horizontal axis (from Equation 14), this means that the resultant displacement is ~90° to the ENA, i.e. the final beam displacement is perpendicular to the ENA; a result consistent with the symmetric cross-section case. This last statement corroborates the fact that for symmetric cross-sections, the elastic curve represents the ENA curvature (BEER *et al*., 2006).

The finite element model (FEM) displacements were very close (5.95% difference) to those obtained by the differential equations integration by Runge-Kutta. Therefore, in a Serviceability Limit State, and from a design view point, the elastic curve integration by Runge-Kutta is validated with the finite element model adopted.

Acknowledgements

The author acknowledges the Universidade Comunitária da Região de Chapecó (Unochapecó) and the Universidade Federal do Rio Grande do Sul (UFRGS) for technical and scientific support.

References

BATHE, K. J. ***Finite element procedures.*** (2. ed.) USA: Prentice-Hall, 1996.

BEER, F. P., JOHNSTON JR., E. R., DeWOLF, J. T. ***Resistência dos materiais: mecânica dos materiais.*** (4. ed). McGraw-Hill, 2006.

BURDEN, R. L., FAIRES, J. D. ***Análise Numérica.*** (2 ed.). São Paulo: Cengage Learning, 2013. (Trad. All Tasks).

KREYSZIG, E., ***Matemática superior para engenharia.*** (9. ed). Rio de Janeiro: LTC, 2009. v. 1. (Trad. Luís Antonio Fajardo Pontes).

MARTHA, L. F. ***Análise de estruturas: conceitos e métodos básicos.*** Rio de Janeiro: Elsevier, 2010.

ODEN, J. T., RIPPERGER, E. A. ***Mechanics of elastic structures.*** (2. ed.). McGraw-Hill, 1981.

PRESS, W. H., TEUKOLSKY, S. A., VETTERLING, W. T., FLANNERY, B. P. ***Numerical recipes: the art of scientific computing.*** (3 ed.). New York: Cambridge University Press, 2007.

SORIANO, H. L., LIMA, S. S. ***Análise de estruturas: método das forças e método dos deslocamentos.*** (2. ed.). Rio de Janeiro: Editora Ciência Moderna Ltda, 2006.

Received: 18 May 2018 - Accepted: 21 December 2018.